

# Densification inhibitor of low-dielectric binary glass composite

JAU-HO JEAN, J.-I. SHEN

*Department of Materials Science and Engineering, National Tsing Hua University, Hsinchu, Taiwan*

The effect of gallium oxide on densification of low-dielectric binary glass composite containing a low-softening-point borosilicate glass (BSG) and a high-softening-point high silica glass (HSG) has been investigated. By doping 2–10 vol% gallium oxide into the binary glass composite, the densification is dramatically reduced, but the activation energy of densification at a given densification is significantly increased. The above results are attributed to an interfacial reaction between alkali ions from low-softening-point BSG and gallium ion from gallium oxide. The interfacial reaction takes place at the interface of BSG and gallium oxide and forms a reaction layer with a composition rich in alkali and gallium ions, which continuously reduces the alkali ion content in the BSG and causes a rise in the viscosity of BSG during firing. Because the rate-limiting step during densification of the binary borosilicate glass is the viscous flow of BSG, a higher viscosity of BSG slows down the densification kinetics and increases the activation energy of densification.

## 1. Introduction

To meet the demands of very large-scale of integration (VLSI), ceramic substrates for advanced electronic packages are decreasing in dielectric constant to increase signal propagation speed [1]. Moreover, a match in thermal expansion coefficient between the ceramic substrate and the active chip is desired to remove design constraint and reliability concerns of electronic packages [2]. To develop a glass composite meeting the above requirements, several approaches, including glass-ceramics [3] and glass + ceramics [4–8] have been taken. The starting materials used in the glass-ceramics approach is pure glass, such as cordierite glass [3] which densifies first, followed by crystallization. The physical properties of the resulting composite in the glass-ceramics approach are controlled by the degree of crystallization. For the glass + ceramics approach, the low-softening point glass acts as densification flux to enhance densification and the ceramic fillers, to adjust the physical properties of the resulting composite. Because of its simplicity and ease in controlling densification behaviour and tailoring physical properties of the resulting composite, the glass + ceramics approach has been widely used [4–8] and is also used in this study.

In a previous investigation [9], a low dielectric constant ( $k = 3.8$ – $4.0$  at 1 MHz) binary glass composite containing a low-softening-point borosilicate glass (BSG), a high-softening-point high silica glass (HSG) was developed. However, a sintering experiment on the above binary glass composite indicated the formation of a crystalline phase of cristobalite that resulted in a large thermal expansion coefficient and made the structure mechanically weak. Microstruc-

tural and thermal expansion results further suggested that the devitrification originated in HSG rather than in BSG [10]. Devitrification results showed that the devitrification process exhibited a characteristic incubation time which decreased with increasing sintering temperature. Activation energy analysis suggested that the rate-limiting step during devitrification was the transport kinetics of alkali ions from BSG to HSG.

In another investigation on the densification of the low-dielectric binary glass mixture of BSG and HSG [11], it was found that the densification was nearly complete prior to the onset of cristobalite formation, suggesting that the crystallization played little role on densification. We further found that the densification was controlled by viscous flow of pure BSG when the sintered density was below a critical value and by viscous flow of silica-rich (reacted) BSG when the density was above the critical value. In addition, the critical density value increased with increasing BSG content in the mixture.

It was later found that the cristobalite formation in the binary glass mixture of BSG and HSG could be prevented by incorporating a crystal growth inhibitor such as gallium oxide [12]. The above results were attributed to a strong coupling reaction between alkali ions from BSG and gallium ion from  $\text{Ga}_2\text{O}_3$ , thus causing a diversion in the transport of alkali ions from HSG to  $\text{Ga}_2\text{O}_3$ . Experimental results [13] also showed that the above compositions containing BSG, HSG and gallium oxide had a dielectric constant in the range 4–6 at 1 MHz and a thermal expansion coefficient in the range of  $3$ – $5 \times 10^{-6} \text{ K}^{-1}$  at 20–200 °C.

Having thus obtained a cristobalite-free low-*k* glass composite, it is necessary to investigate the effect of the interfacial reaction between alkali ions from BSG and gallium ion from gallium oxide on the densification kinetics and the mechanism of the low-dielectric binary glass composite before the composition to obtain desirable properties is optimized. Therefore, effects of gallium oxide content and sintering temperature on densification kinetics and the mechanism of the binary glass composition of BSG and HSG were studied in this investigation.

## 2. Experimental procedure

As-received borosilicate glass (BSG) (Corning code 7070), high silica glass (HSG) (Corning code 7913) and gallium oxide powders were used in this study. The low-softening-point BSG powder had a composition of 70–75 wt % SiO<sub>2</sub>, 20–25 wt % B<sub>2</sub>O<sub>3</sub> and trace amounts of Li<sub>2</sub>O, Na<sub>2</sub>O and K<sub>2</sub>O; the high-softening-point HSG had a composition of 95 wt % SiO<sub>2</sub>, 4 wt % B<sub>2</sub>O<sub>3</sub> and a trace amount of Al<sub>2</sub>O<sub>3</sub>, and the crystalline gallium oxide had > 99 wt % Ga<sub>2</sub>O<sub>3</sub>. In addition, the BSG and HSG had softening points of 700–750, and > 1500 °C, respectively. Particle-size distributions of the powders were determined by sedimentation, and the results showed that the glass powders had a median size of 7 μm and gallium oxide, 2–3 μm. X-ray diffraction analysis showed that the as-received glass powders were amorphous, and gallium oxide exhibited the beta phase.

The powders were mixed with 5 wt % poly(ethylene glycol) binder in 1-propanol. The suspension was deagglomerated by a high-energy ultrasonic probe, and mixing was continued using a Turbula mixer (Maschinenfabrik Basel, Switzerland) for 2 h. The powder mixture was dried, ground, and uniaxially pressed at about 90 MPa to make pellets of 1.3 cm diameter and 0.3 cm high. The density of the green compacts was determined dimensionally and used to describe densification behaviour. Samples were then sintered isothermally in air at 850–925 °C for various periods of time. They were pushed into the heating zone after binder burn-out at 500 °C for 1 h. A period of 3 min was allowed for the samples to equilibrate at the sintering temperatures. After completion of sintering, the samples were air-quenched to room temperature. No cracks were visually observed. Sintered densities were measured by the water replacement method. Samples were immersed in water, and the open pores were filled with water in vacuum for 2 h. The theoretical densities of 2.13 g cm<sup>-3</sup> for BSG, 2.18 g cm<sup>-3</sup> for HSG and 5.95 g cm<sup>-3</sup> for gallium oxide, were used to calculate the theoretical densities of the glass composite by using the rule of mixtures. The microstructure of the sintered compact was taken from fractured and polished surfaces using a scanning electron microscopy (SEM), and compositional analysis was determined with wavelength dispersion spectroscopy in a microprobe.

Because the composition of 40 vol % BSG–60 vol % HSG was used for previous devitrification and densification studies [4, 11, 14], we continued to use

it as a model composition for this investigation. To reveal the effect of gallium oxide on densification of the low-dielectric binary borosilicate glass composite, a direct substitution of gallium oxide for an equivalent amount of HSG was made. The major reason for this substitution was due to the fact that the low softening point BSG acts as a densification flux during sintering, and a 40 vol % BSG can ensure a high sintered density for the samples used for physical property measurements.

## 3. Results

The densification factor (DF) which represents the porosity removed during densification is used to describe the densification behaviour and is defined as [15]

$$DF = (D_s - D_g)/(D_{th} - D_g) \quad (1)$$

where  $D_s$  is the instantaneous sintered density,  $D_g$  is the green density, and  $D_{th}$  is the theoretical density of the composite calculated by the rule of mixtures. Although the green density of the compacts after binder burn-out should be used in Equation 1, there is difficulty in obtaining reliable densities because of its fragility, and hence we used the density of the as-pressed compacts.

Typical densification results for the samples with gallium oxide contents from 0–10 vol %, fired at 875 °C, are shown in Fig. 1. For gallium oxide-free sample, the densification increases rapidly initially, slows down and then stops at a constant densification factor. The gallium oxide-doped samples, however, exhibit two stages of densification: a rapid increase initially, followed by an even slow rise in densification. It is also noted that a slower and smaller densification factor is always observed with a greater amount of gallium oxide content. Similar phenomena are also observed at other temperatures from 850–925 °C. Thus, the addition of gallium oxide to the low dielectric binary glass mixture of BSG and HSG inhibits not only the formation of cristobalite [12], but also achieving densification. A negative DF is noticed in Fig. 1 at the early stage of densification. This is due to the fact that the green density of the as-pressed compact is used and the densification is insufficiently large to compensate for the density reduction after the binder was removed from the green compact.

Fig. 2 shows the effect of sintering temperature on densification for the samples with 10 vol % gallium oxide fired at 850–925 °C. A similar densification pattern is observed for all temperatures investigated; i.e. the densification increases rapidly initially and then slows down. As expected, a faster and larger densification is observed at a higher temperature. The same phenomenon is also observed for other gallium oxide contents from 2–10 vol %.

Fig. 3 summarizes the results of densification factor at 240 min for all temperatures and gallium oxide contents investigated. It was found that the densification factor decreases with increasing gallium oxide content at a given sintering temperature. Unlike the gallium oxide-free sample where the densification

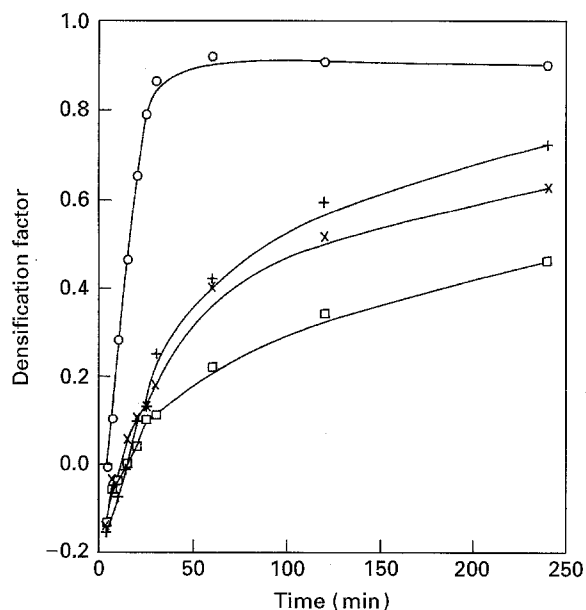


Figure 1 Densification factor as a function of time for the samples with (○) 0, (+) 2, (×) 5 and (□) 10 vol % gallium oxide fired at 875 °C.

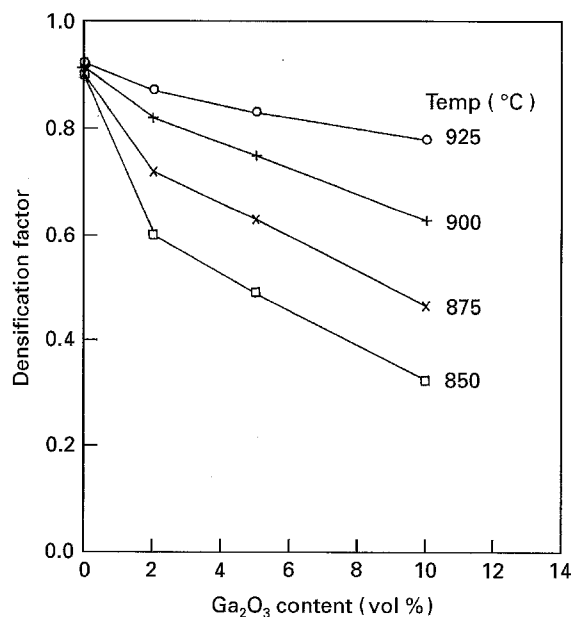


Figure 3 Densification factor at 850–925 °C for 240 min as a function of gallium oxide content.

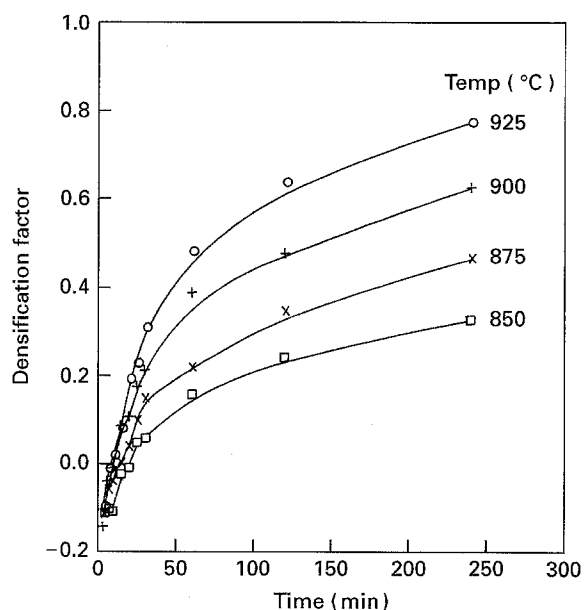


Figure 2 Densification factor versus time for the sample with 10 vol % gallium oxide fired at 850–925 °C.

shows little dependence on temperature, the densification factor of gallium oxide-doped sample increased with increasing sintering temperature and the dependence became more significant as the gallium oxide content increased.

The instantaneous densification rate as a function of densification factor at various temperatures from 850–925 °C for the samples with 0, 2, 5 and 10 vol % gallium oxide are presented in Fig. 4a–d, respectively. The instantaneous densification rate is calculated by differentiating a curve-fitting equation to the experimental densification factor–time plots (Fig. 1). It is found in Fig. 4 that the densification rate decreases linearly with increasing densification factor, and the dependence, characterized by the slope of the curve, decreases with decreasing temperature. At a given

densification factor, moreover, a larger densification rate is observed at a higher sintering temperature for all compositions investigated. Comparing the results in Fig. 4a for gallium oxide-free sample with Fig. 4b–d for gallium oxide-doped samples at a given sintering temperatures, a larger densification rate is always observed for the gallium oxide-free sample. This is further evidenced by the results shown in Fig. 5, in which the instantaneous densification rate at an arbitrary densification factor, e.g. 0.3, is plotted as a function of gallium oxide content. It follows further that a smaller instantaneous densification rate is observed with an increase in gallium oxide content.

The above results on the reduction of densification by the addition of gallium oxide is also supported by comparing the microstructures of the gallium oxide-free sample with that of a gallium oxide-added sample, e.g. 10 vol %, as shown in Fig. 6a and b, respectively. Both samples had been fired at 925 °C for 240 min, and the micrographs were taken from fracture surfaces. Dense and uniform microstructure with few isolated pores and a relative density greater than 98% is observed for the gallium oxide-free sample. However, the porous microstructure of the gallium oxide-doped sample shows large continuous pores and a low density of 90%, indicating a poor densification.

#### 4. Discussion

The results presented in Figs 1–6 clearly indicate that the densification of the low-dielectric binary glass mixture is retarded with 2–10 vol % gallium oxide present. These results can be explained by a strong coupling reaction between  $\text{Ga}^{3+}$  from gallium oxide and alkali ions from BSG, as shown in Fig. 7. Fig. 7a shows a typical scanning electron micrograph for the sample with 5 vol % gallium oxide fired at 900 °C for 8 h, along with elemental mapping of  $\text{Ga}^{3+}$  (Fig. 7b),  $\text{K}^+$  (Fig. 7c), and  $\text{Si}^{4+}$  (Fig. 7d). Clearly, the  $\text{Ga}^{3+}$

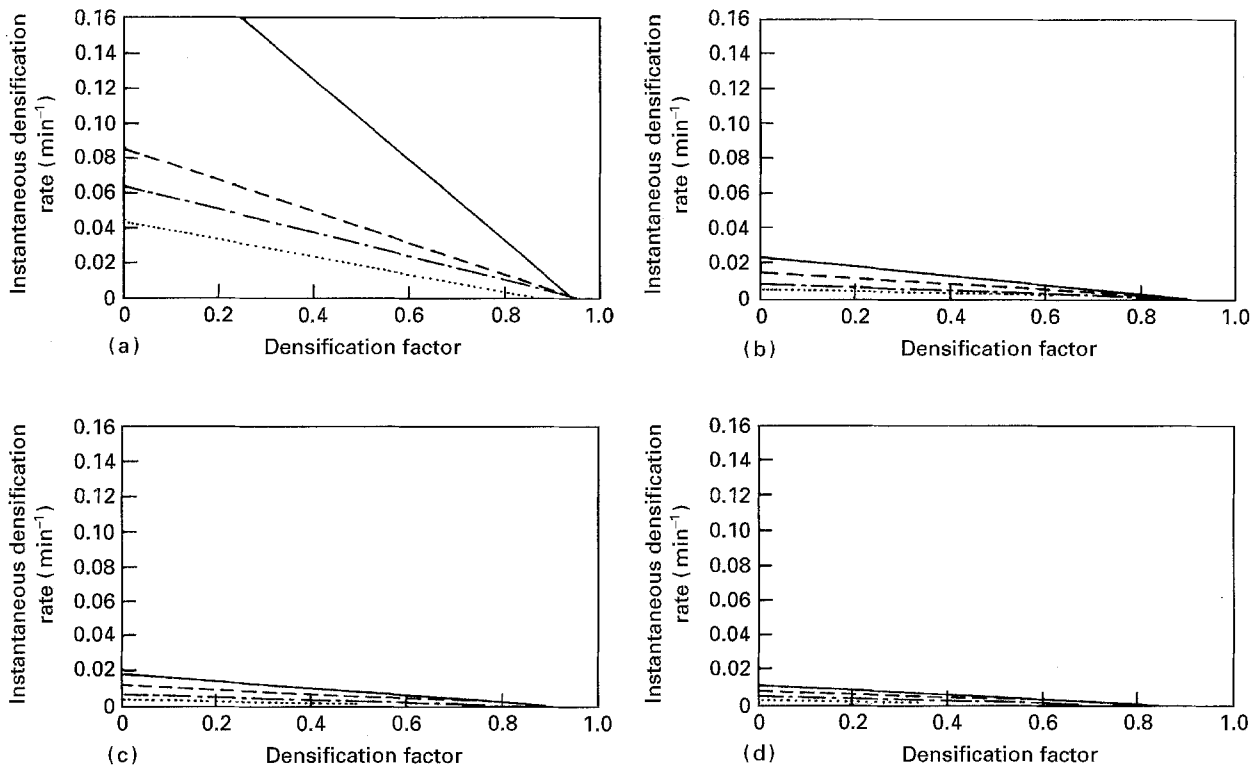


Figure 4 Instantaneous densification rate versus densification factor for the samples with various gallium oxide contents: (a) 0, (b) 2, (c) 5 and (d) 10 vol %. (···) 850 °C, (---) 875 °C, (---) 900 °C, (—) 925 °C.

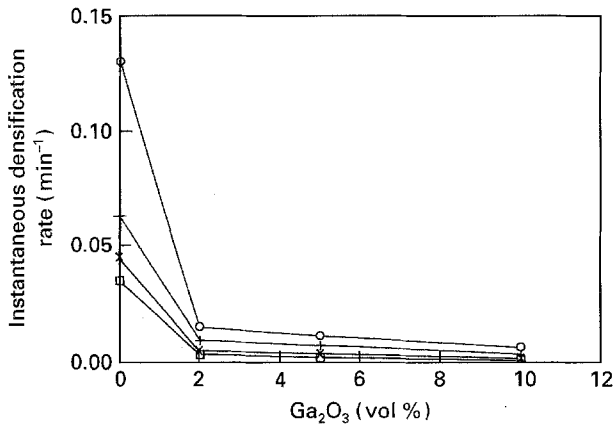


Figure 5 Instantaneous densification rate at DF = 0.3 versus gallium oxide content. (○) 925 °C, (+) 900 °C, (×) 875 °C, (□) 850 °C.

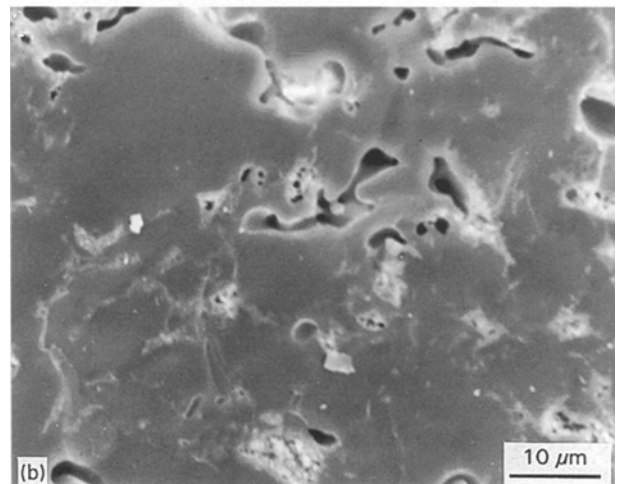
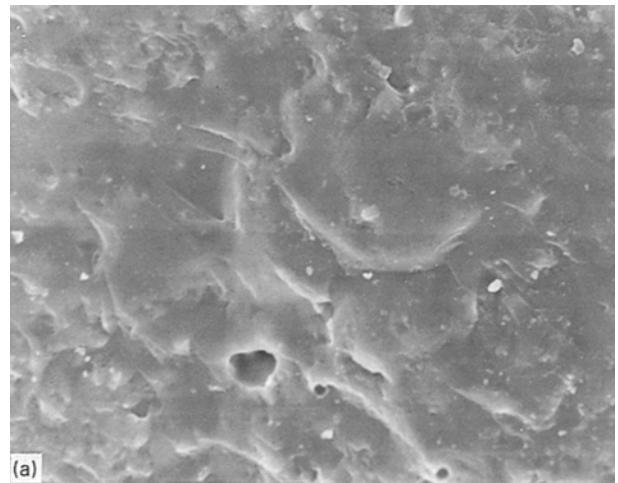


Figure 6 Scanning electron micrographs for the samples with (a) 0 and (b) 10 vol % gallium oxide fired at 925 °C for 240 min.

from gallium oxide and  $K^+$  from BSG are strongly coupled and exhibit the same geometric configuration in the microstructure. The above result is further evidenced in a kinetic study of interfacial reaction between BSG and gallium oxide substrate, as shown in Fig. 8 [12]. Because the above reaction between BSG and gallium oxide promotes a continuous migration of the alkali ions from BSG to the interface of gallium oxide particles during sintering, it correspondingly depletes the concentration of alkali ions in BSG. Accordingly, the resultant loss of alkali ions from BSG will raise the viscosity of the BSG [16], causing a significant reduction in densification kinetics because the densification is mostly controlled by viscous flow of the low-softening BSG [13] at the sintering temperatures investigated. For the systems with gallium oxide, a smaller and slower densification is observed

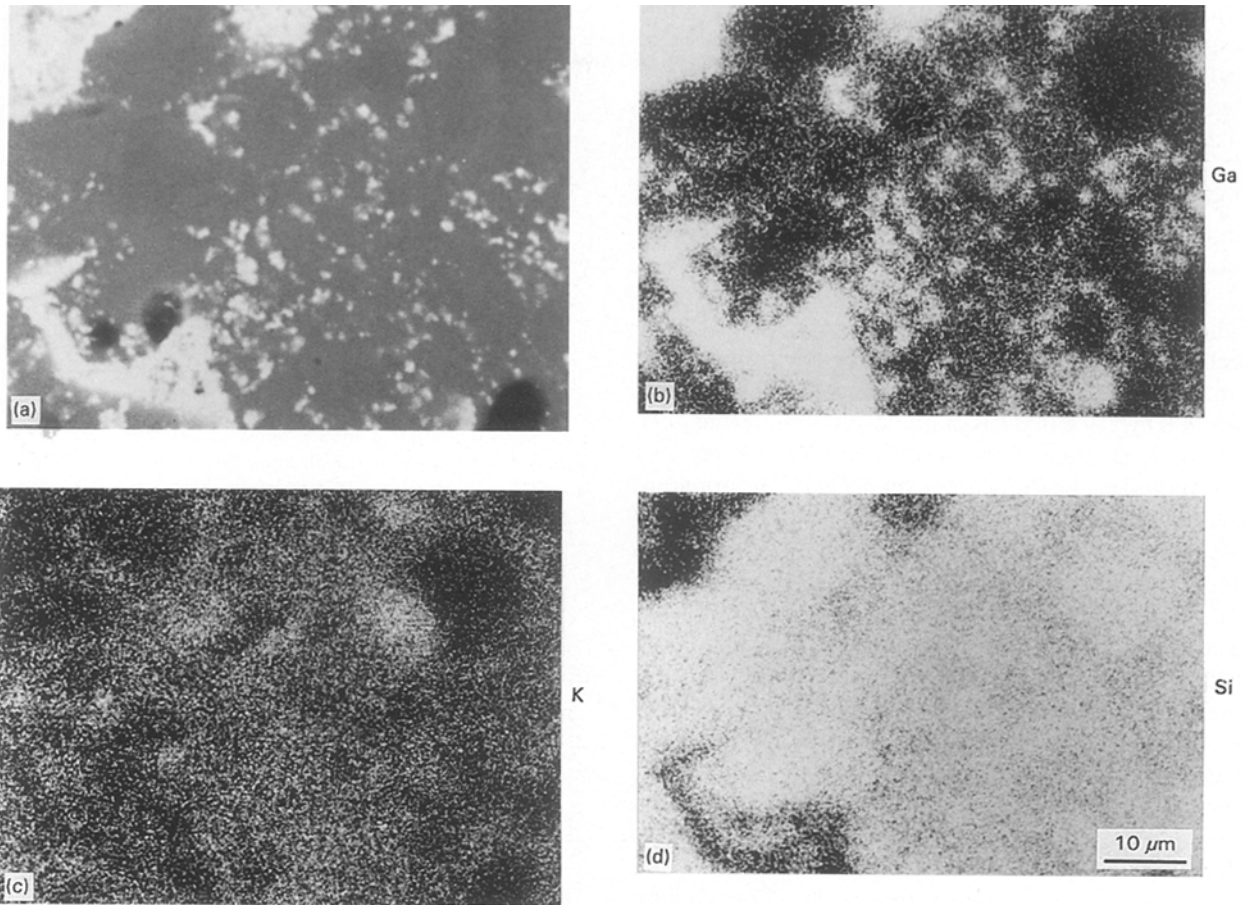


Figure 7 (a) Back-scattering electron image of a sample with 5 vol % gallium oxide, and elemental mapping of (b) gallium, (c) potassium, and (d) silicon fired at 900 °C for 480 min.

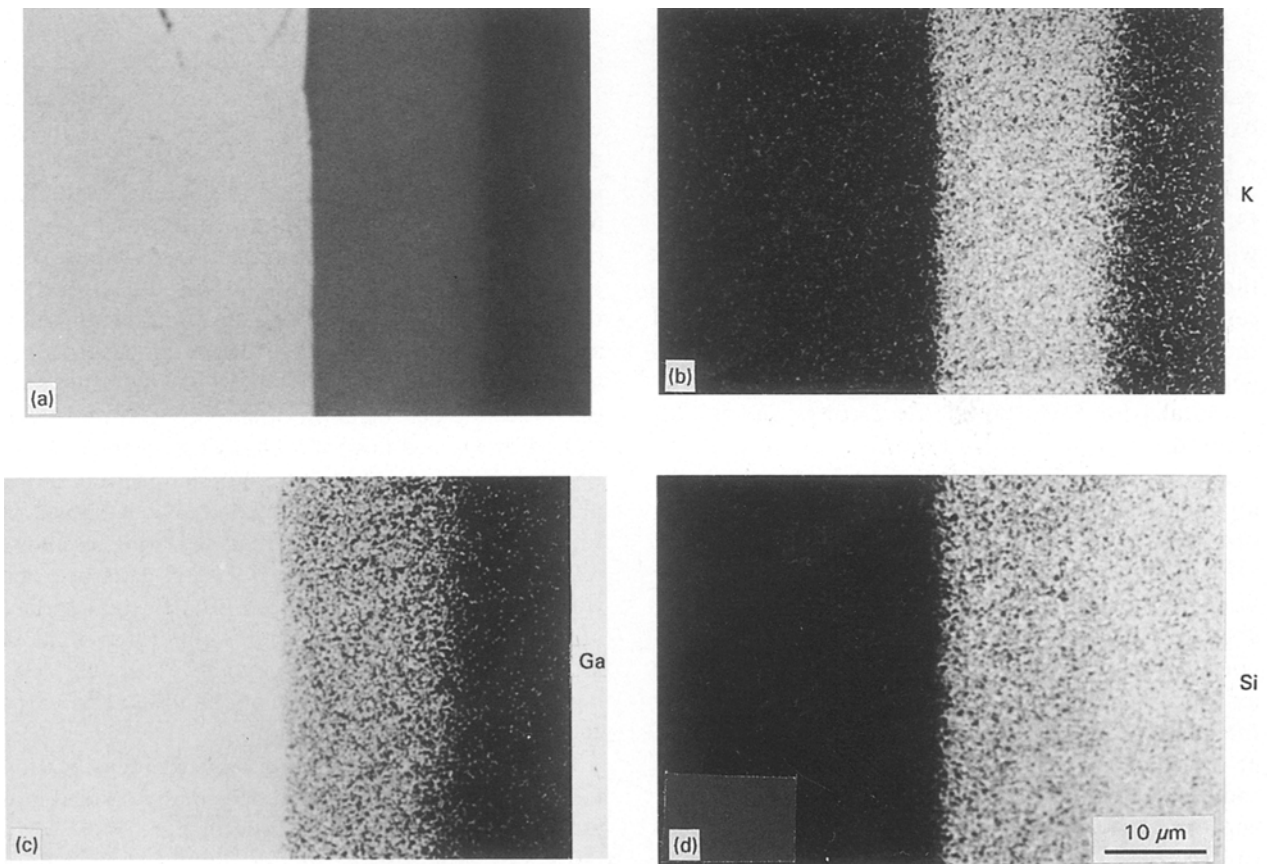


Figure 8 (a) Back-scattering electron image of a diffusion couple between gallium oxide and BSG fired at 900 °C for 240 min, and elemental mapping of (b) potassium, (c) gallium, and (d) silicon.

with an increase in gallium oxide content. This can be explained by the fact that the total surface area of gallium oxide available for the coupling reaction between alkali ions from BSG and  $\text{Ga}^{3+}$  from gallium oxide increases with increasing gallium oxide content. This enhances the chemical reaction kinetics between BSG and gallium oxide, causing a significant increase in the viscosity of BSG and thus resulting in a reduction in densification.

To determine the rate-controlling step during densification, the apparent activation energy of the kinetically controlled process needs to be determined from an Arrhenius plot. The plots are constructed, based upon Kingery's analysis of liquid-phase sintering [17], as the logarithm of the specific rate ( $T\partial DF/\partial t$ ) at a constant densification factor versus  $1/T$ . The apparent activation energies are then determined from the slopes by a least-squares fit method. Fig. 9 presents typical results at  $DF = 0.1$ – $0.45$  for the sample with 10 vol % gallium oxide. Straight lines are observed, and the slope of these lines increases gradually with increasing densification factor, suggesting an increased apparent activation energy with increasing densification factor. Similar results are also observed for other gallium oxide contents investigated, and are further supported by the results of apparent activation energy as a function of densification factor in the curves of Fig. 10b–d for the system with 2, 5, and 10 vol % gallium oxide, respectively. For gallium oxide-free sample [11], the result of the apparent activation energy versus densification factor is presented in Fig. 10a. Furthermore, the activation energies for viscous flow of BSG [13] and HSG [13] are also included in Fig. 10 for comparison.

For a given densification factor, the apparent activation energy increases with increasing gallium oxide content. At a given gallium oxide content, moreover, the apparent activation energy initially exhibits a plateau with increasing DF, but increases appreciably with DF when the DF reaches a critical value,  $DF^*$ . The magnitude of the plateau increases slightly with increasing gallium oxide content. However, the value of  $DF^*$ , which is determined from the intercept of two arbitrary slopes, one from the plateau and the other from the rapidly rising portion, increases with decreasing gallium oxide content; i.e. 0.3 for 10 vol %, 0.4 for 5 vol %, 0.5 for 2 vol % and 0.7 for 0 vol %.

For the gallium oxide-free sample (Fig. 10a), the apparent activation energy initially remains relatively unchanged in the range  $240$ – $250 \text{ kJ mol}^{-1}$  at  $DF < DF^*$ . The above values are close to that for viscous flow of pure BSG ( $220$ – $240 \text{ kJ mol}^{-1}$  [13]), suggesting that the densification is controlled by viscous flow of pure BSG. For  $DF > DF^*$ , however, the activation energy increases gradually with increasing DF from  $270 \text{ kJ mol}^{-1}$  at  $DF = 0.7$  to  $380 \text{ kJ mol}^{-1}$  at  $DF = 0.85$ . Because these values are in between those for viscous flow of pure BSG and HSG, it suggests that the predominant densification mechanism in these regions is likely to be viscous flow of a changing composition (reacted) BSG, resulting from the continuous dissolution of HSG in BSG [11].

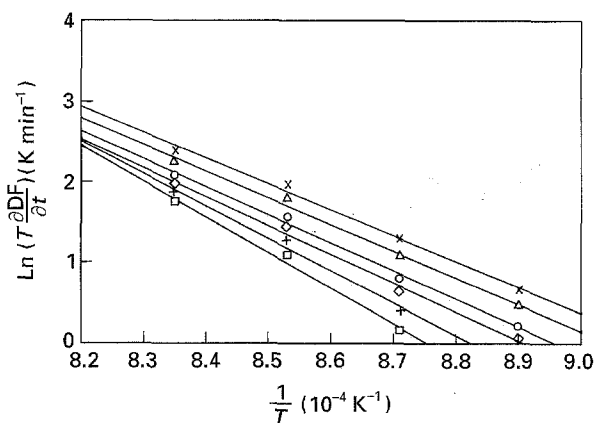


Figure 9 Logarithm of specific densification rate [ $\ln(T\partial DF/\partial t)$ ] versus  $1/T$  at a given densification factor for the sample with 10 vol % gallium oxide. DF: (x) 0.1, ( $\Delta$ ) 0.2, ( $\circ$ ) 0.3, ( $\diamond$ ) 0.35, (+) 0.4, ( $\square$ ) 0.45.

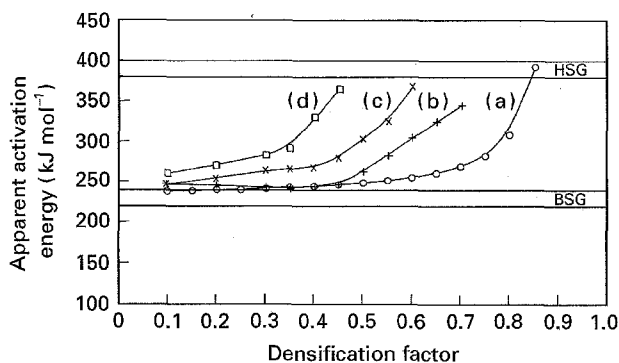


Figure 10 Apparent activation energy as a function of DF for the samples with (a) 0, (b) 2, (c) 5 and (d) 10 vol % gallium oxide, and activation energies for viscous flow of BSG [13] and HSG [13].

For the gallium oxide-doped samples with  $DF < DF^*$  (Fig. 10b–d), the apparent activation energies of densification are in the range  $230$ – $260 \text{ kJ mol}^{-1}$ , and are very close to that for viscous flow of pure BSG,  $220$ – $240 \text{ kJ mol}^{-1}$  [13]. The above result suggests that the densification of glass composite under these conditions is most likely controlled by viscous flow of pure BSG. It follows further that for the conditions with  $DF > DF^*$ , the apparent activation energies are within the range governed by viscous flow of both BSG and HSG. This result suggests that the densification of glass composite is controlled by viscous flow of a changing composition of BSG which is formed by the coupling reaction taking place between gallium oxide and BSG as shown in Figs 7 and 8. As stated earlier, a strong coupling reaction takes place between BSG and gallium oxide which migrates alkali ions from BSG to the interface of the BSG/gallium oxide. The resultant loss of alkali ions in BSG causes a rise in viscosity [16], thus slowing down the densification kinetics and increasing the activation energy of densification.

Based upon the above discussion, the densification kinetics of this composite can be broadly divided into two stages: mostly viscous flow of pure BSG when  $DF < DF^*$  and mostly viscous flow of reacted BSG when  $DF > DF^*$ . Therefore,  $DF^*$  represents the highest densification achievable by viscous flow of

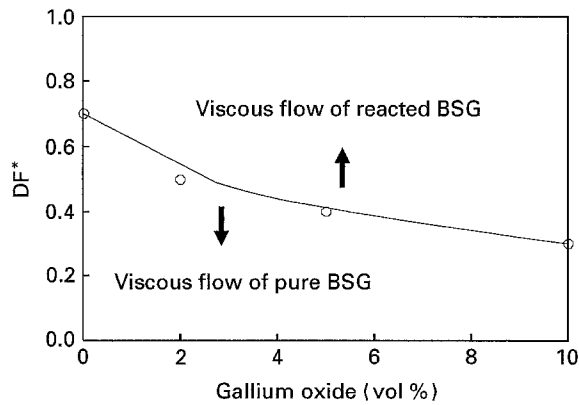


Figure 11 DF\* versus gallium oxide content.

pure BSG. With this definition, a plot of DF\* versus gallium oxide then separates the viscous flow of the pure BSG stage from the viscous flow of the reacted BSG stage, as shown in Fig. 11. As stated earlier, a greater DF\* value is observed with a smaller amount of gallium oxide, which is explained by the interfacial reaction taking place between BSG and gallium oxide (Figs 8 and 9).

## 5. Conclusion

The effect of gallium oxide on densification of low-dielectric binary borosilicate glass containing a low softening point borosilicate glass (BSG) and a high softening point high silica glass (HSG) has been investigated. It is found that the addition of gallium oxide to the low-dielectric binary glass composite significantly slows down the densification kinetics, but increases the activation energy of densification. The above result is explained by a strong coupling reaction taking place between BSG and gallium oxide during sintering. The interfacial reaction migrates the alkali ions from BSG to the interface of BSG and gallium oxide, which continuously reduces the alkali ions content in BSG, thus increasing the viscosity of BSG and slowing down the densification kinetics of the glass composite.

## Acknowledgements

The technical assistance of Chia-Ruey Chang is greatly appreciated. Funding for this study was provided by the National Science Council, Taiwan, under Grant NSC-85-2221-E-007-045.

## References

1. R. R. TUMMALA, *J. Am. Ceram. Soc.* **74** (1991) 895.
2. *Idem*, in "Microelectronic Packaging Handbook", edited by R. R. Tummala and E. J. Rymaszewski (Van Nostrand Reinhold, New York, 1989) Ch. 7.
3. H. C. BHEDWAR and H. T. SAWHILL, in "Electronic Materials Handbook", Vol. 1 (ASM International, Cleveland, OH, 1989) p. 455.
4. K. NIWA, Y. IMANAKA, N. KAMEHARA and S. AOKI, in "Advances in Ceramics", Vol. 26, edited by M. F. Yan, K. Niwa, H. M. O'Bryan Jr and W. S. Young (American Ceramic Society, Westerville, OH, 1988) p. 323.
5. K. KATA, Y. SHIMADA and H. TAKAMIZOWA, *IEEE Trans. CHMT* **13** (1990) 448.
6. J. I. STEINBERG, S. J. HOROWITZ and R. J. BACHER, in "Advances in Ceramics", Vol. 19, edited by J. B. Blum and W. R. Cannon (American Ceramic Society, Westerville, OH, 1986) p. 31.
7. Y. IMANAKA, S. AOKI, N. KAMEHARA and K. NIWA, *J. Ceram. Soc. Jpn Int. Edn* **95** (1987) 1066.
8. D. M. MATTOX, S. R. GURKOVICH, J. A. OLENICK and K. M. MASON, *Ceram. Eng. Sci. Proc.* **9** (1988) 1567.
9. J.-H. JEAN and T. K. GUPTA, *J. Mater. Res.* **7** (1992) 3103.
10. T. K. GUPTA and J.-H. JEAN, *ibid.* **9** (1994) 999.
11. J.-H. JEAN and T. K. GUPTA, *ibid.* **9** (1994) 486.
12. *Idem*, *ibid.* **8** (1993) 2393.
13. W. EPSE, "Materials of High Vacuum Technology", Vol. 2 (Pergamon Press, Oxford, 1968) Ch. 10.
14. J.-H. JEAN and T.-H. KUAN, *Jpn J. Appl. Phys.* **34** (1995) 1901.
15. H. S. CANNON and F. V. LENEL, in "Proceedings of the Plansee Seminar", edited by F. Benesovsky (Metallwerk Plansee, Reutte, 1953) p. 106.
16. W. D. KINGERY, H. K. BOWEN and D. R. UHLMANN, "Introduction to Ceramics", 2nd Edn (Wiley, New York, 1976) Ch. 4.
17. W. D. KINGERY, *J. Appl. Phys.* **30** (1959) 301.

Received 8 August

and accepted 21 December 1995